Egyptian Geophysical Society
EGS Journal, vol. 3, No. 1, 173-184 (2005)

PETROPHYSICAL FACIES DISCRIMINATION OF MIOCENE CALCAREOUS SANDSTONES, WADI FEIRAN, SINAI, EGYPT

Mohamed A. Ragab, Bassem S. Nabawy and Khaled S. Gharib*

Geophysical Sciences Department, National Research Centre, Cairo, Egypt
** Geology Department, Faculty of Science, Zagazig University*

تمييز السحنات البتروفيزيائية للحجر الرملى الجيرى التابع لعصر الميوسين بوادى فيران، سيناء، مصر

الخلاصة: تم إجراء تحليل بتروفيزيائى كامل لعينات من الحجر الرملى الكلسى والتى تم جمعها من منطقة جبل هداهد بوادى فيران – جنوب غرب سيناء. والعينات الصخرية المدروسة تنتمى لعصر الميوسين السفلى (متكون روديس، ٣٣٨,٨ متر) وهو يعلو متكون نُخل فى توافق تام بينما تعلوه طبقات من الحصى والرمال التابعة للعصر الرباعى فى عدم توافق واضح. وصخور الميوسين موضع الدراسة تتكون غالباً من أحجار رملية متداخلة مع طبقات طينية وبعض الأحجار الرملية عند القاعدة. وقد تكونت الصخور المدروسة فى بيئات نهرية وبيئات خليطة من النهرية والهوائية. أما بالنسبة للصفات التخزينية لهذه الصخور فقد تدنت فى بعض النطاقات بسبب التلاحم خاصة بالكالسيت ونادراً ما يكون بالسيليكا وأكاسيد الحديد.

ولقد تم إخضاع العينات الصخرية المدروسة لقياسات بتروفيزيائية كاملة مثل قياس الكثافة الكلية والمسامية والنفاذية وتقدير كمية المحتوى المائي غير القابل للاسترجاع، والالتوائية الكهربية، المقاومة الكهربية الظاهرية عند ثلاثة تشبعات ملحية (٦ و ٦٠ و ١٢٠ ألف جزء في المليون) كما تم كذلك قياس المقاومة الكهربية الحقيقية. ولقد اتاح التحليل البيتروفيزيائي تمييز ثلاث سحنات بتروفيزيائية، السحنتان السفلية والوسطى منها (الجزء السفلي والأوسط من تكون روديس) تتميزان بخصائص تخزينية جيده نتيجة تميزها بقيم عالية من المسامية والنفاذية، بينما السحنة الثالثة (الجزء العلوي من تكون روديس) تتميز بخصائص تخزينية ضعيفة.

ABSTRACT: *Systematic petrophysical studies were carried out on some calcareous sandstone samples selected from Gebel Hadahid area, Wadi Feiran, south west Sinai,. The studied rock samples are belonging to the Lower Miocene (Rudeis Formation, 338.8 m) which conformably overlies the Nukhul Formation and unconformably underlies Quaternary gravels and sands. The Lower Miocene rocks of the studied area are composed mainly of sandstones intercalated with shale beds and few sandy limestone intercalations at the base. The studied samples were deposited in a fluviatile and mixed aeolian-fluviatile environment. The storage capacity of the studied rocks was diminished by cementation, mostly by calcite cementation, and rarely by hematite or silica cement.*

The collected samples were subjected to comprehensive systematic petrophysical investigations including measuring of the bulk density, the porosity, permeability, irreducible water saturation, electric tortuosity of channels, apparent electric resistivity of samples saturated with NaCl solution of three successive concentrations (6, 60, and 120 kppm), and the true electric resistivity. The petrophysical analysis enabled distinguishing three petrophysical facies. The lower and middle facies (lower and middle parts of Rudeis Formation) have good storage capacity properties due to their high porosity and permeability values, whereas the third facies (topmost parts of Rudeis Formation) has fair storage capacity properties.

INTRODUCTION

The Miocene sediments in the Gulf of Suez region represent one of the main hydrocarbon reservoir rocks in Egypt. The majority of oil fields in the Gulf of Suez are producing from the Lower Miocene reservoir rocks, whereas the Middle Miocene evaporites represent excellent cap rocks. These Miocene rocks are widely distributed all over the northern part of Egypt, either on the surface or in the subsurface. The Miocene sediments in the Gulf of Suez had been studied by many authors including Stainforth (1949), Heybroeak (1965), Sadek (1968), El Kerdany (1976), El Heiny (1982), Rateb (1988), Hamza (1988), Arafa (1992), Abu El Enain and Gharib (1997), and others.

The present study aims to throw some light on the storage capacity properties of the Lower Miocene Rudeis clastics at Gebel Hadahid to establish its reliability as reservoir or aquifer rocks in its subsurface equivalent extensions.

Studying of surface exposures equivalent to the target subsurface reservoir rocks is a fast and cheap exploratory tool and helps to investigate the petrophysical properties and their vertical and horizontal variation with large number of samples and also offer the capability of resampling for further studies, which is not available in the subsurface studies.

Gebel Hadahid area is located in the western part of central Sinai, between latitudes $28^{O}35'$ & $28^{O}45'$ N and longitudes $33^{O}20'$ & $33^{O}25'$ E. It is bounded from the North and North West by Wadi Feiran (Fig. 1). Therefore, a set of representative fresh samples were collected from the calcareous sandstone beds of Rudeis

Formation at Gebel Hadahid, and prepared in the geophysical lab. in the National Research Centre, Giza, to clarify their petrophysical properties.

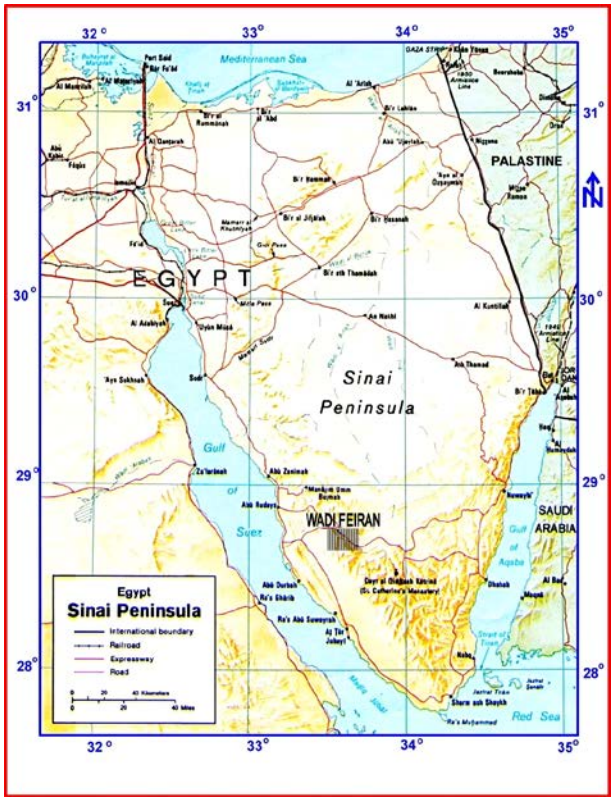

Fig. 1: Location map of Gebel Hadahid area, Wadi Feiran, South West Sinai, Egypt.

METHODS AND TECHNIQUES

The collected rock samples were drilled and prepared for the petrophysical measurements as plugs of 2.5 cm diameter and 2.5 cm length. Further, the core samples were cleaned from soluble salt contents, and dried in an electric oven up to 90^{O}C as a maximum temperature. The applied methods and techniques were carried out in the Department of Geophysics, National Research Centre.

The insoluble residue analysis and decantation method, introduced by McQueen (1931) and Ireland (1958), using dilute HCl is applied to the rest of the core samples to determine carbonate, mud and sand fraction percentages. These components define to some extent the rock type and explain its petrophysical behaviour.

Several methods have been used by different authors for porosity determination. In laboratory measurements, it is necessary to determine only two of three volumes namely: the bulk volume, interconnected pore volume and grain volume. The saturation method introduced by Koithara et al. (1968) is used in the present work for measuring both the porosity and the bulk density of the studied core samples. The method is based on determination of the pore volume and the bulk volume. Gas permeability measurements (K, md) were carried out using Ruska gas permeameter (Amyx et al., 1960) in the Exploration Department of the Egyptian Petroleum Research Institute (EPRI).

The pore channel diameter (D) of the studied samples was calculated for each sample using the equation offered by Rzhevsky & Novik (1971) as follows:

$$D = (32\ K / \varnothing)^{0.5}$$

where; K = Permeability, in μm^2; and

$\varnothing$ = Porosity, %.

The irreducible water saturation (S_{wirr}) was measured using the high speed centrifuge method, Janetzki-T32A apparatus outlined by Koithara et al. (1968), where the samples were saturated with distilled water (ρ_f = 1.0) and further desaturated for a time period of fifteen minutes and were weighed, and then the process was repeated as a cycle till reaching a constant weight, W_{ds} (Ragab et al., 1999), then the following equation was applied to the measured weights:

$$S_{wirr} = [(W_{ds} - W_d) / (W_s - W_d)]$$

where, W_{ds} : the weight of the desaturated sample,

W_d : the weight of the dry sample, and

W_s : the weight of the saturated sample.

After that, the electrical resistivity measurements were carried out on the core samples by using A-C Bridge (model TF-2700) at three successive cycles of brine saturations (6, 60, and 120 kppm) with NaCl solutions (R_w = 0.93 ohm.m, 0.21 ohm.m, and 0.11 ohm.m, respectively) to investigate the effect of the conductive solids. The true electric resistivity (R_t) of the core samples is measured at the last stage of desaturation while the irreducible water saturation S_{wirr} of the brine solution was 6 kppm. (Parkhomenko, 1967; Gür, 1976; El Sayed and Zeidan, 1983; Ragab et al., 2000). The formation resistivity factor was calculated for each rock sample at each concentration, as:

$$F = R_o / R_w \qquad \text{(Amyx et al., 1960)}$$

Values of the electric tortuosity factor (T) of the studied rocks were calculated for the first formation resistivity factor using the following equation (Gür, 1976; Ragab et al., 2000):

$$T = (F \times \varnothing)^{0.5} \qquad \text{(Gür, 1976)}$$

Lithostratigraphy and Petrography

The Rudeis Formation in the studied area represents a clastic section which overlies the Nukhul Formation and underlies unconformably the Quaternary gravels and sands.

According to Abu ElEnain and Gharib (1997), the majority of the Rudeis sandstones are medium-grained,

few sandstone intercalations are fine to coarse grained. The relationship between the grain size parameters indicates river and/or mixed river and dune sediments with some exceptional beach sediments. The studied Rudeis section attains 338.8 m at Gebel Hadahid and consists mainly of yellowish to brown sandstones, well bedded, cross-bedded, hard to moderately hard, highly calcareous, argillaceous in parts, slightly pebbly (Plate 1, Figs. A & B) and ferruginous at the upper parts (Plate 1, Fig. C).

The base of the Rudeis Formation is characterized by 22.8 m of grey to yellow, moderately hard sandy clayey fossiliferous limestone. Figure (2) shows a composite lithostratigraphic column of the surface Lower Miocene Rudeis Formation in Gebel Hadahid area.

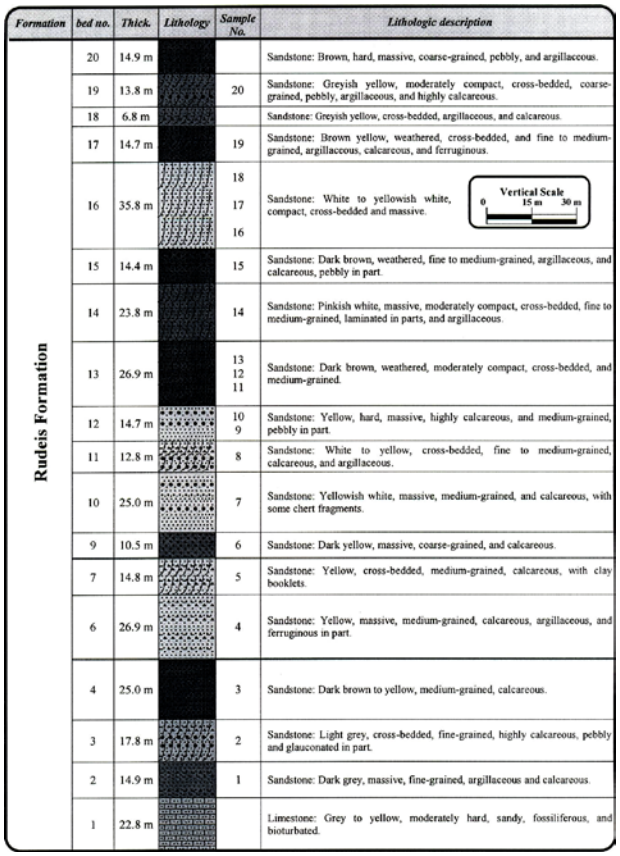

Fig. 2: A composite lithostratigraphic column of the surface Lower Miocene Rudeis Formation, Gebel Hadahid, Wadi Feiran, South West Sinai (After Abu El Enain and Gharib, 1997).

From the petrographic study, the investigated samples could be divided into quartz arenite (88 %) and quartz wacke (12 %) facies. The quartz arenite facies are subdivided into: lithic quartz arenite, siliceous quartz arenite, ferruginous quartz arenite, and calcareous quartz arenite, whereas the wacke facies is represented by the quartz wacke (Abu ElEnain and Gharib, 1997). The calcareous quartz arenite facies represents most of the studied rock samples of the Rudeis Formation in Hadahid area.

Moreover, many physical and chemical diagenetic processes diminished the porosity of the Rudeis rock samples. The physical processes are represented mainly by compaction and pressure solution, whereas the chemical processes are represented mainly by cementation (mostly by calcite (Plate 1, Figs. A & B), rarely by silica and iron oxides), replacement, and neomorphism. On the other side, corrosion, and dissolution of the quartz grains (Plate 1, Fig. D) enhance the porosity values.

RESULTS AND DISCUSSION

The studied calcareous sandstone samples of Rudeis Formation (Lower Miocene age) are divided into 3 petrophysical facies forming all the most parts of Rudeis Formation according to their density, storage capacity properties and the electric behaviour (Table 1).

Facies (1):

The first facies of the Rudeis calcareous sandstone which represents the lower part (150.2 m) of the formation, is composed mainly of sand grains (average 59.70 %), carbonate (average 32.50 %) and low clay content (average 7.8 %). It is characterized by porosity values (∅) lie between 10.06 % (σb = 2.44 g/cm^3) and 12.13 % (σb = 1.91 g/cm^3) with an average 11.13 % (medium ∅). The permeability values range from 2.47 md to 16.38 md with an average 9.38 md (permeable). The values of bulk density (σb) lying between 1.91 and 2.44 g/cm^3 with an average of 2.24 g/cm^3. The apparent electric resistivity measurements (R_o) range from 167.65 ohm.m (σb =1.98 g/cm^3, ∅ = 12.03 %, T = 4.66) to 994.4 ohm.m (σb = 2.44 g/cm^3, ∅ = 10.06 %, T = 10.37) with an average of 480.1 ohm.m. On the other side, the true electric resistivity results (R_t) lie between 1534.3 and 2761.6 ohm.m with an average of 2151.7 ohm.m, whereas the electric tortuosity values vary from 4.66 to 10.4 averaging 7.18. The pore channel diameter varies from 0.92 μm up to 2.07 μm with an average of 1.54 μm.

The porosity is inversely proportional to the bulk density (r = -0.738, Fig. 3a) and to the electric tortuosity of channels (r = -0.907, Fig. 3b), while the permeability is mainly affected by the porosity (r = 0.966, Fig. 4a) and also by the electric tortuosity of channels (r = -0.800, Fig. 4b).

$$\sigma b = -0.16 \varnothing + 3.98 \quad (r = -0.74)$$
$$T = -2.14 \varnothing - 31.1 \quad (r = -0.95)$$
$$\text{Log } K = 8.15 \text{ Log } \varnothing - 7.6 \quad (r = 0.97)$$
$$\text{Log } K = -0.12\, T + 1.7 \quad (r = -0.80)$$

The porosity values are not affected by the variation in the mineralogic composition of the studied rocks ($r \leq 0.30$), whereas the coefficients of variation of the main mineralogic components are 0.110 for both the

sand and carbonate fractions. Values of the formation resistivity factor at the different concentrations depend mainly on the porosity (r ≥ -0.91, Figs. 5a, b, c & d), whereas the apparent electric resistivity values are dependent mainly on the true electric resistivity (r = 0.788, Fig. 5d) and on the electric tortuosity of channels (r = –0.996, Fig. 6a).

$\text{Log } F_{0.21} = -7.8 \text{ Log } \varnothing + 11.5$ (r = –0.92)

$\text{Log } F_{0.11} = -7.99 \text{ Log } \varnothing + 11.9$ (r = –0.91)

$\text{Log } R_t = 0.24 \text{ Log } R_o - 2.7$ (r = 0.79)

$T = 7.2 \text{ Log } R_1 - 11.5$ (r = 0.99)

Plate 1

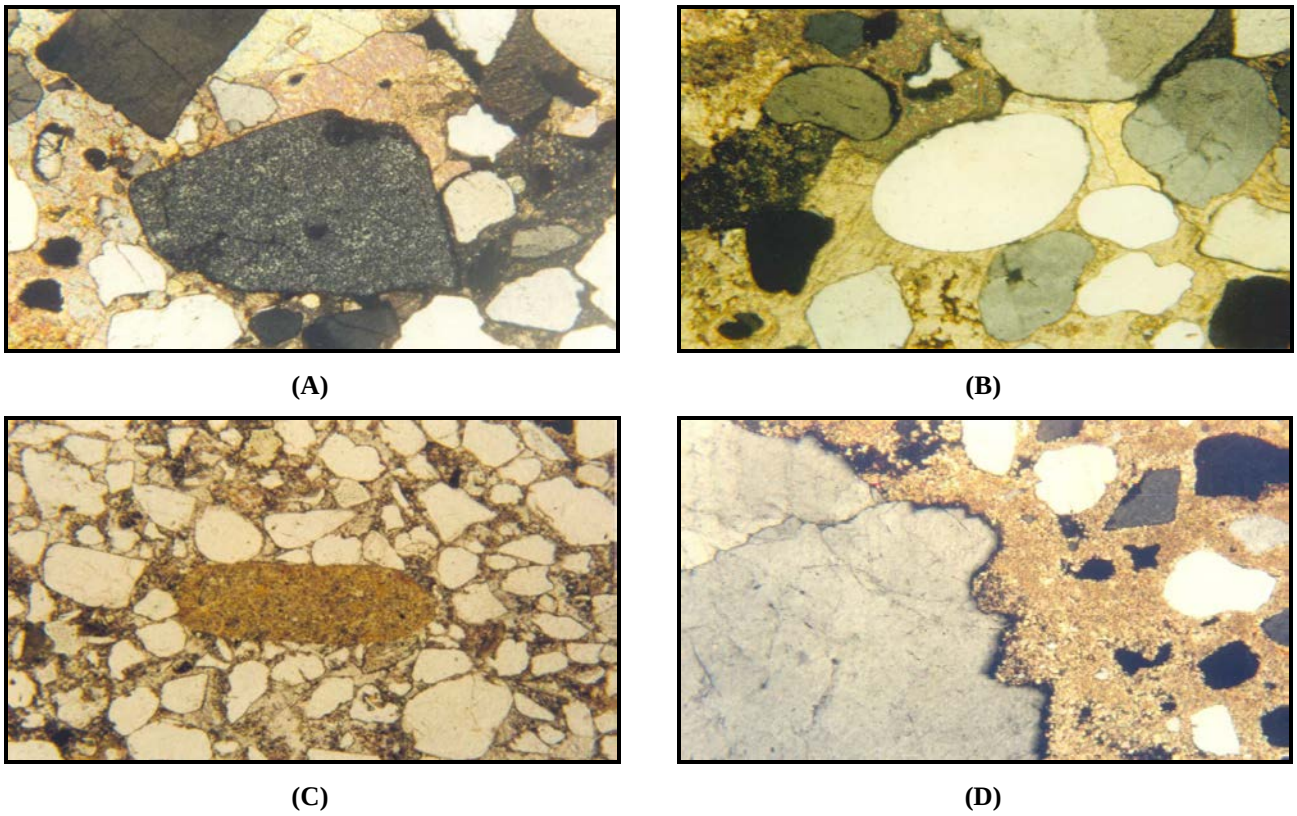

(A) **(B)**

(C) **(D)**

Fig. A: Photmomicrograph showing pebbly lithic quartz arenite embedded in well developed sparry calcite cement, C.N., X 100, sample no. 15, Fig. B: Photmomicrograph of calcareous quartz arenite showing tight cementation with sparry calcite cement, C.N., X 100, sample no. 12, Fig. C: Photomicrgraph showing ferruginated quartz arenite with phosphatic grain, PPL, X 50, Sample no. 4, Fig. D: Photmomicrograph showing pebbly sandstones showing the corrosion and partial dissolution of the pebbly quartz grain by the cement, C.N., X 50, sample no. 20.

From the formation resistivity factors data at the three concentrations, there is no lime-mud effects for samples of Facies 1, where the value of $F_{0.93} < F_{0.21} < F_{0.11}$ (Table 1). The pore channel diameter is reasonably inversely proportional to the electric tortuosity (r = –0.830, Fig. 7a), whereas it is directly proportional to the permeability values (r = 0.999, Fig. 7b).

$T = -3.77 \text{ D} - 13.04$ (r = –0.83)

$\text{Log K} = 1.08 \text{ Ln D} + 0.47$ (r = 0.99)

$\text{Log } F_{0.93} = -7.6 \text{ Log } \varnothing + 10.6$ (r = –0.92)

Facies (2):

The second facies of the calcareous sandstone rock samples (middle part of the Rudeis Formation, 65.4 m) is composed mainly of sand grains (average 68.1 %), carbonate (average 26.9 %) and negligible mud fraction (average 4.9 %). It is characterized by very good porosity lies between 15.1 % (σb = 2.62 g/cm^3) and 24.91 % (σb = 2.12 g/cm^3) with an average 19.9 %.

Results of the permeability measurements range from 40.6 md (∅ = 16.0 % & T = 16.7) to 557.3 md (∅ = 24.9 % & T = 19.0) with an average of 192 md. The σb values lie between 2.12 & 2.62 g/cm^3 with an average 2.39.

The Ro measurements range from 1353 (σb = 2.12 g/cm^3, ∅ = 24.91 %, T = 19.0) and 1725 ohm.m (σb = 2.62 g/cm^3, T = 16.7), while values of the R_t measurements lie between 2700 ohm.m (S_{wirr} = 25.83 %) and 3780 ohm.m (S_{wirr} = 18.4 %). The electric tortuosity values vary from 16.7 to 19.0 with an average of 18.1. The pore channel diameter varies from 2.8 μm up to 8.4 μm with average 4.9 μm.

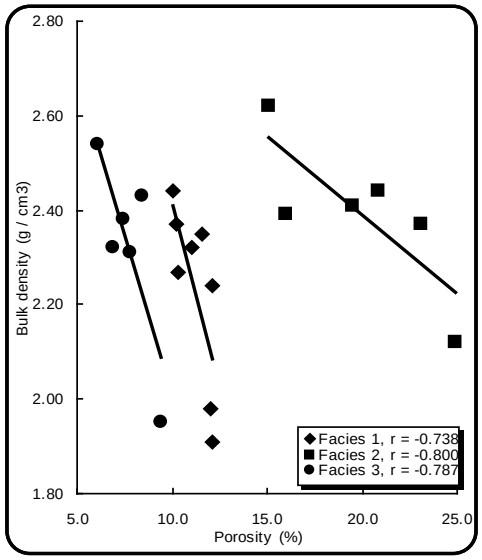

(a)

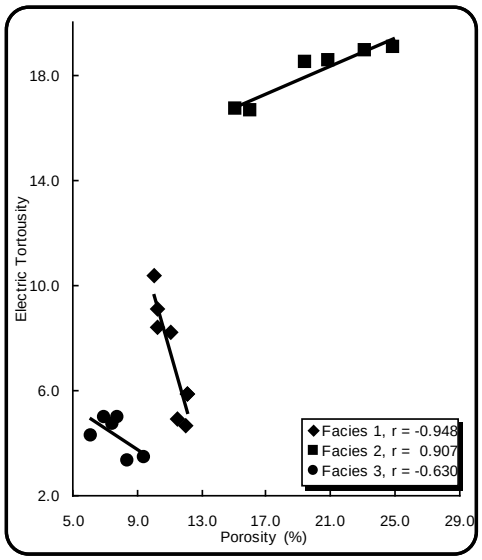

(b)

Fig. 3: The relationship between the porosity and both of: a) bulk density; and b) electric tortuosity of channels (T) of Rudeis Formatio

σb =- 0.03 ∅ + 3.05 (r = –0.80)

T = 0.27 ∅ + 12.8 (r = 0.91)

Carb. (%) = 44.1 ∅ + 83.9 (r = –0.80)

The bulk density is a main contributor of the porosity (r = -0.80, Fig. 3a), whereas the electric tortuosity of channels is directly proportional to the porosity (r = 0.91, Fig. 3b). The porosity values are also controlled by the mineralogic composition (r = 0.435), where it is inversely related to the carbonate cement content (r = –0.798, Fig. 6b) and directly related to the sand content (r = 0.62).

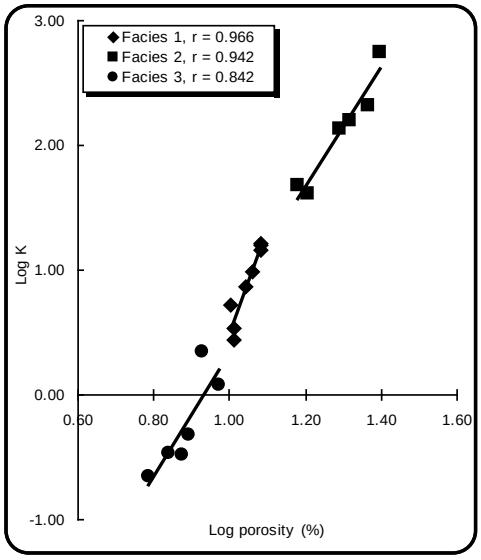

(a)

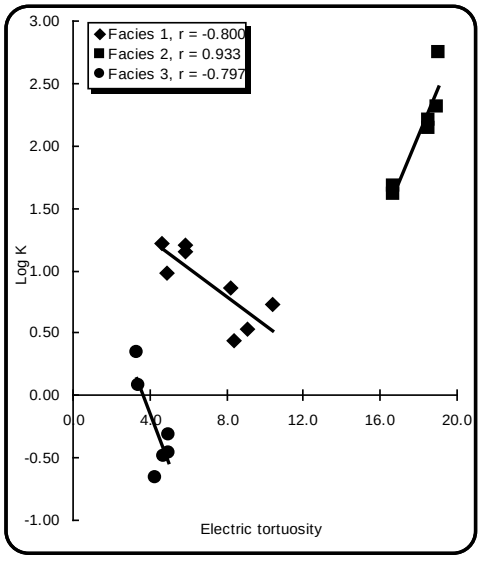

(b)

Fig. 4: The relationship between the permeability and: a) the porosity; and b) the electric tortuosity of channels (T) of Rudeis Formation.

The permeability is mainly affected by the porosity (r = 0.94, Fig. 4a) and is related to the electric tortuosity of channels in a direct proportional relationship (r = 0.93, Fig. 4b). The formation resistivity factor values at the different concentrations depend on the porosity (r > -0.91, Figs. 5a, b & c).

$$\text{Log K} = 4.72 \text{ Log } \varnothing - 3.98 \quad (r = 0.94)$$

$$\text{Log K} = 0.36 \text{ T} - 4.46 \quad (r = 0.93)$$

$$\text{Log } F_{0.93} = -0.41 \text{ Log } \varnothing + 3.8 \quad (r = -0.92)$$

$$\text{Log } F_{0.21} = -0.410 \text{ Log } \varnothing + 4.39 \quad (r = -0.91)$$

$$\text{Log } F_{0.11} = -0.411 \text{ Log } \varnothing + 4.67 \quad (r = -0.91)$$

According to the values of the formation resistivity factor at the three concentrations, there are no lime-mud effects in samples of Facies 2 (Table 1). The electric tortuosity of channels is inversely related to the apparent electric resistivity (r = -0.79, Fig. 6a), and directly related to the pore channel diameter (r = 0. 804, Fig. 7a), whereas the pore channel diameter is directly related to the permeability values of the rock samples (r = 0. 998,

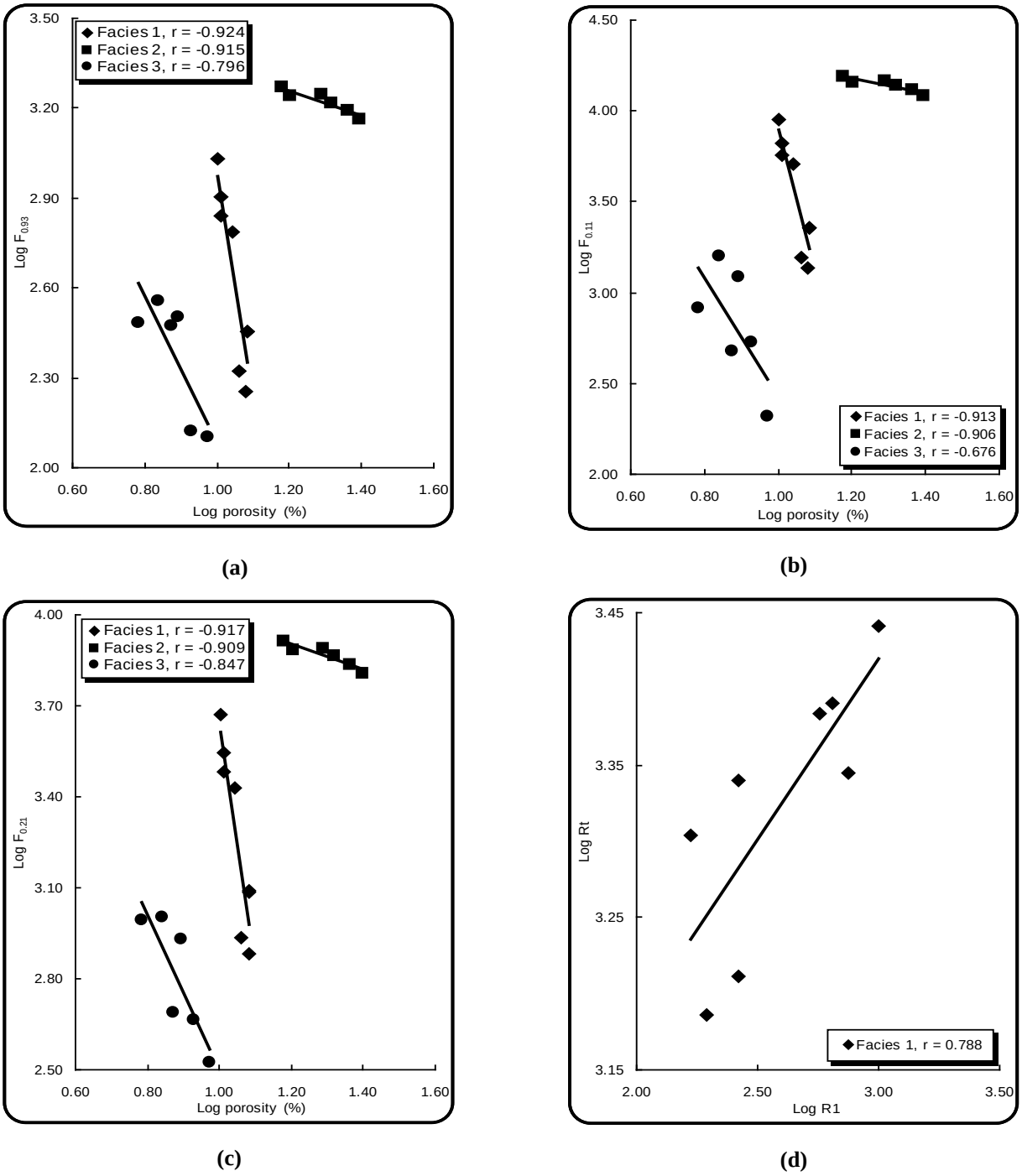

Fig. 5: The dependence of the formation resistivity factor on the porosity values at concentrations: a) 6000 ppm, b) 60000, and c) 120000 of the studied Rudeis samples, whereas d) the dependence of the apparent electric resistivity values of the first facies on the true electric resistivity.

Fig. 7b), i.e., in the same time the electric tortuosity increases with increasing the pore channel diameter and therefore, the permeability and porosity increase.

$T = -22.2 \text{ Log } R_1 - 89.1$ (r = 0.79)

$T = 0.45 D - 15.85$ (r = 0.80)

$\text{Log } K = 0.97 \text{ Ln } D + 0.5$ (r = 0.99)

Facies (3):

The third facies of the studied calcareous sandstones represents the uppermost parts of Rudeis Formation (100.4 m). It is composed mainly of sand grains (average 55.56 %), carbonate (average 38.42 %) and low mud fraction (average 9.36 %). It has low ∅ ranging from 6.09 % ($\sigma b = 2.54$ g/cm^3) up to 9.40 % ($\sigma b = 1.95$ g/cm^3) with an average of 7.69 %. The bulk density values lie between 1.95 (∅ = 9.4 %) and 2.54 g/cm^3 (∅ = 6.1 %) with an average of 2.32 g/cm^3. The permeability values range from 0.22 md (T = 4.30) to 2.23 md (T = 3.35) with an average of 0.80 md. The Ro measurement values lie between 117 ohm.m (σb = 1.95 g/cm^3, ∅ = 9.4 %, T = 3.44) and 333.8 ohm.m (σb = 2.32 g/cm^3, ∅ = 6.91 %, T = 4.98), while the R_t values lie between 535 ohm.m (S_{wirr} = 27.0 %) and 3510 ohm.m (S_{wirr} = 41.9 %). The electric tortuosity values range from 3.35 to 5.00, averaging 4.30. The pore channel diameter varies from 0.34 μm up to 0.91 μm with an average 0.52 μm.

The bulk density is mainly contributed by the porosity values (r = –0.79, Fig. 3a), whereas the porosity is a main contributor of the electric tortuosity factor (r = –0.63, Fig. 3b).

The porosity values have not been affected by the mineralogic composition of the studied rocks (r < 0.497), where the Coefficient of Variation equals 0.25 for the sand content, and 0.08 for the carbonate fraction.

$\sigma b = - 0.135 \varnothing + 3.367$ (r = -0.79)

$T = - 0.40 \varnothing + 7.40$ (r = -0.63)

The permeability is mainly affected by the porosity (r = 0.84, Fig. 4a) and by the electric tortuosity of channels (r = –0.797, Fig. 4b). The formation resistivity factor measurement values at the different concentrations depend mainly on the porosity values (r ≥ -0.68, Figs. 5a, b & c). The lime-mud effect is observed at the second and third saturations, where the values of $F_{0.21} > F_{0.11}$ at samples no. 15, 18 and 19.

$\text{Log } K = 4.90 \text{ Log } \varnothing - 4.6$ (r = 0.84)

$\text{Log } K = - 0.41 T - 1.5$ (r = -0.80)

$\text{Log } F_{0.93} = - 2.47 \text{ Log } \varnothing + 4.6$ (r = -0.80)

(Coefficient of Variation = Standard deviation/ mean)

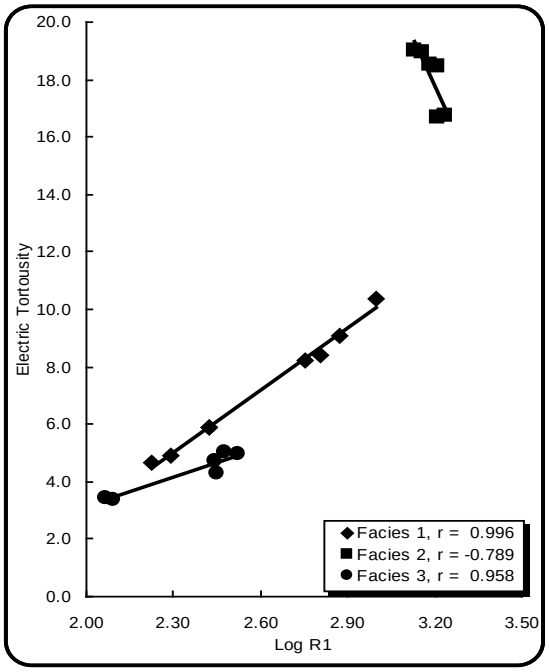

(a)

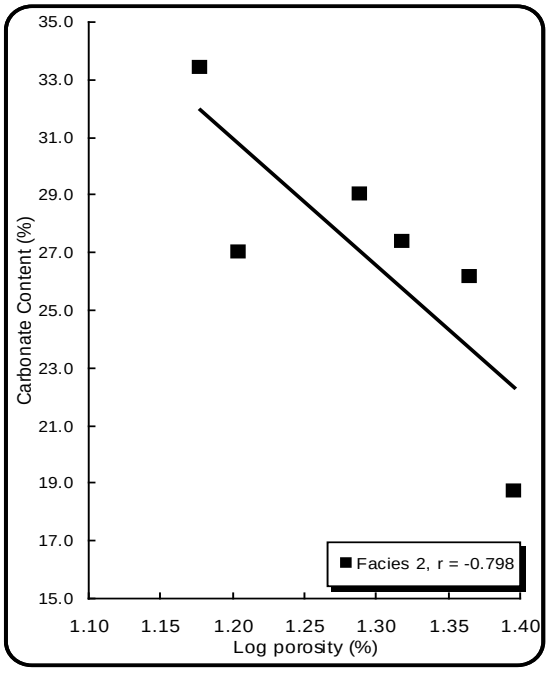

(b)

Fig. 6: The relationship between:

a) The apparent electric resistivity and the electric tortuosity of channels of the different facies; and

b) The porosity and the carbonate content of the second facies (middle parts of Rudeis Formation).

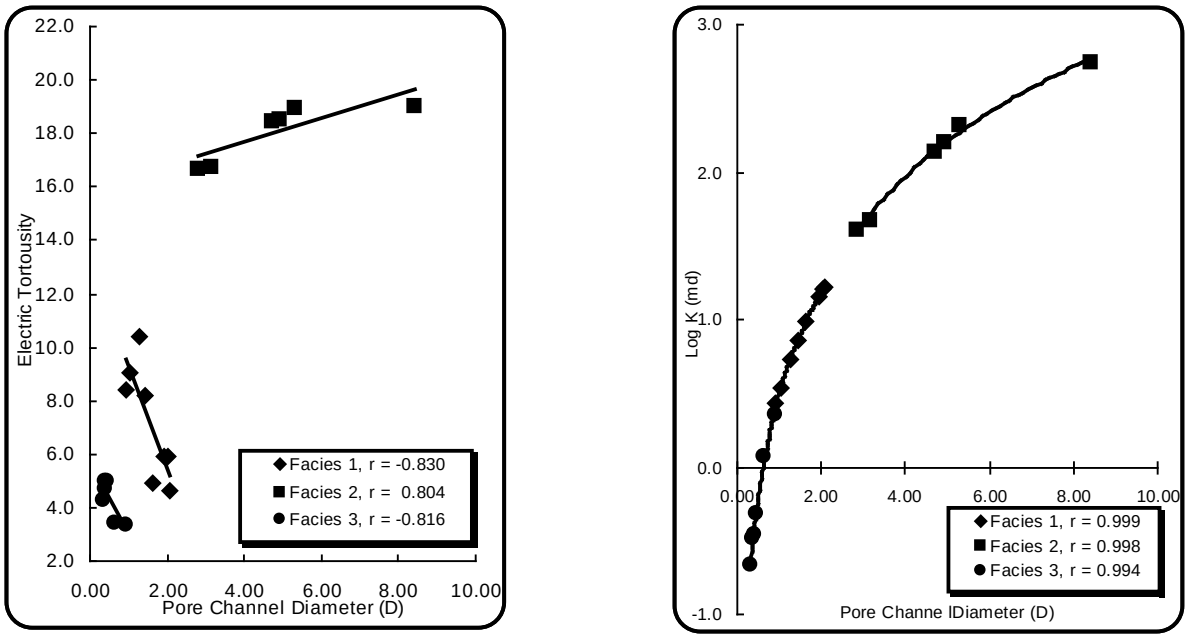

(a) **(b)**

Fig. 7: The relationship between the pore channel diameter and: a) the electric tortuosity of channels; and b) the permeability of the different facies of Rudeis Formation.

$$\text{Log } F_{0.21} = -2.57 \text{ Log } \varnothing + 5.06 \qquad (r = -0.85)$$

$$\text{Log } F_{0.11} = -3.25 \text{ Log } \varnothing + 5.69 \qquad (r = -0.68)$$

Therefore, the weak anomaly in the electric behaviour of Facies 3 (the correlation coefficient of the F-∅ relationship is between $-0.847 \geq r \geq -0.68$) could be attributed to the lime mud effect in some samples. The apparent electric resistivity values are dependent mainly on the electric tortuosity of channels (r = 0.96, Fig. 6a).

$$T = 3.49 \text{ Log } R_1 - 3.87 \qquad (r = 0.96)$$

The pore channel diameter is reasonably inversely proportional to the electric tortuosity (r = –0.816, Fig. 7a), whereas it is directly proportional to the permeability values (r = 0.994, Fig. 7b). The following equations could be applied to the petrophysical parameter relations of the third facies (the uppermost parts of Rudeis Formation):

$$T = -2.75 \text{ D} - 5.72 \qquad (r = -0.82)$$

$$\text{Log K} = 1.00 \text{ Ln D} + 0.48 \qquad (r = 0.99)$$

GENERAL DISCUSSION AND RESERVOIR ZONATION

From the previous discussion, it is established that the petrophysical properties and behaviour is a reliable tool that could be used for discriminating the good storage facies for a given rock sequence. In our study, the petrophysical properties and behaviour were used to discriminate the Rudeis Formation in Wadi Feiran, into the three mentioned petrophysical facies.

Both the lower and middle parts of the Rudeis (the first and second facies of the studied section) have good storage capacity due to their high porosity and permeability, while the uppermost parts (the third facies) has low storage capacity due to their poor porosity and permeability (Table 1). The poor storage capacity of the third facies could be attributed to the well cementation by calcite cement.

In general, the porosity has an inverse relationship with the bulk density (Fig. 3a) and the electric tortuosity of channels (Fig. 3b), while the permeability is mainly affected directly by the porosity (Fig. 4a) and inversely by the electric tortuosity values (Fig. 4b).

$$\sigma b = -0.033 \varnothing + 3.052 \qquad (r = -0.80)$$

$$T = -2.14 \varnothing - 31.06 \qquad (r = -0.95)$$

$$\text{Log K} = 8.15 \text{ Log } \varnothing - 7.64 \qquad (r = 0.97)$$

$$\text{Log K} = 0.36 \text{ T} - 4.46 \qquad (r = 0.93)$$

For the rock samples of Facies number 2, there is some anomaly in the relation between the electric tortuosity of channels and both the porosity and permeability (Figs. 3b, 4b), which could be explained theoretically by the fact that the electric tortuosity is a product vector of both the porosity and the formation resistivity factor. Therefore, the electric tortuosity factor of the rock samples of facies 2 is contributed mainly from increasing the porosity, whereas of samples of

facies 1 & 3 are contributed mainly from the formation resistivity factor. Moreover, with increasing the porosity values, the permeability increases, therefore values of the electric tortuosity factor of samples from facies 2 should reasonably increase. The porosity values are not affected by the variation in the mineralogic composition except for the porosity of facies no. 2 which depends mainly on the carbonate and sand contents (Fig. 6a), i.e. with increasing the cement content of samples from facies 2, the porosity decrease. Both the apparent electric resistivity and the formation resistivity factor values are dependent on the porosity values (Figs. 5a, b & c) and the electric tortuosity of channels (Fig. 6a). The apparent electric resistivity is dependent on the true electric resistivity in the middle parts only (second facies) (Fig. 5d). Taking into consideration the fact that the porosity of the second facies (15.07 % ≤ ∅ ≤ 24.91 %) is a main contributor of the apparent electric resistivity, and that the porosity is mainly dependent on the variation of the mineralogic composition of the second facies, therefore, the dependence of the apparent electric resistivity on the true electric resistivity is a logic result, and vice versa in the other facies.

$$\text{Log } F_{0.93} = -7.62 \text{ Log } \varnothing + 10.61 \quad (r = -0.92)$$

$$\text{Log } F_{0.21} = -7.82 \text{ Log } \varnothing + 11.45 \quad (r = -0.92)$$

$$\text{Log } F_{0.11} = -7.99 \text{ Log } \varnothing + 11.91 \quad (r = -0.91)$$

$$T = 3.49 \text{ Log } R_1 - 3.87 \quad (r = 0.96)$$

In general, there is an inverse relationship between values of the pore channel diameter and the electric tortuosity factor, whereas there is a reasonably direct proportionality between the pore channel diameter and the measured values of permeability.

$$T = -2.75 \text{ D} - 5.72 \quad (r = -0.82)$$

$$\text{Log K} = 1.00 \text{ Ln D} + 0.48 \quad (r = 0.99)$$

The presence of some anomalies in the petrophysical behaviour of the second facies (T versus ∅, T versus K, and T versus R_1) could be attributed to the high electric tortuosity, which increases by increasing the porosity of this facies (Fig. 3b, Table 1). Moreover, another anomaly of the electric tortuosity of samples of facies 2 was recorded for the relation with the pore channel diameter, which suggests a *special case*. Practically, this anomaly for samples of facies 2 could be attributed to increasing both the electric tortuosity (Fig. 7a) and the permeability (Figs. 4b, 7b) with increasing the pore channel diameter at the same time (Fig. 8).

Moreover, according to the similarity of the mineralogic composition and components of the studied facies and according to the highest correlation coefficient, a set of equations of correlation coefficients more than 0.80 were offered relating the different measured petrophysical parameters to each other, these equations could be applied to the studied calcareous sandstones of the surface Lower Miocene Rudeis Formation in Gebel Hadahid, Wadi Feiran.

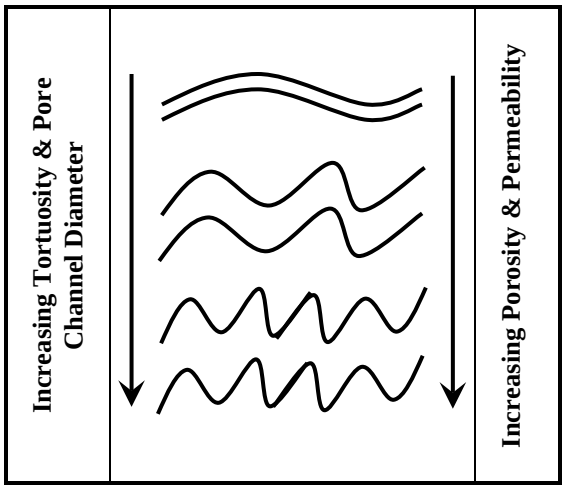

Fig. 8: A sketch showing an explanation of the special case recorded for facies 2, where the electric tortuosity factor increases with increase of the pore channel diameter, and therefore both the porosity and permeability on the other hand increase.

From the present work, the multiplier (a) and the cementation exponent (m) of the different studied facies increase with increasing the salinity of the solution. El Sayed et al. (1999), on the other hand, studied the effect of the overburden pressure on the estimated a & m of the Rudies Formation in Gebel Hadahid area and concluded that both a & m increase with increasing the overburden pressure.

Under some conditions such as similarity of the mineralogic composition, the paleoenvironment and the diagenetic history, and taking the geopressure into considerations, the offered equations could be applied to the subsurface Rudies Formation in the subsurface seeking for different hydrocarbon fluids.

Figure (9) shows a log-chart illustrating the vertical variation of the different petrophysical parameters measured in this study and shows the principles on which the reservoir zonation was carried out. From the chart, it is concluded that both facies 1 & 2 (the lower part of Rudeis Formation in Gebel Hadahid) are accepted as excellent horizons having good storage properties, whereas the third facies (top most parts of the Rudies Formation) is not accepted due to its low grade storage properties.

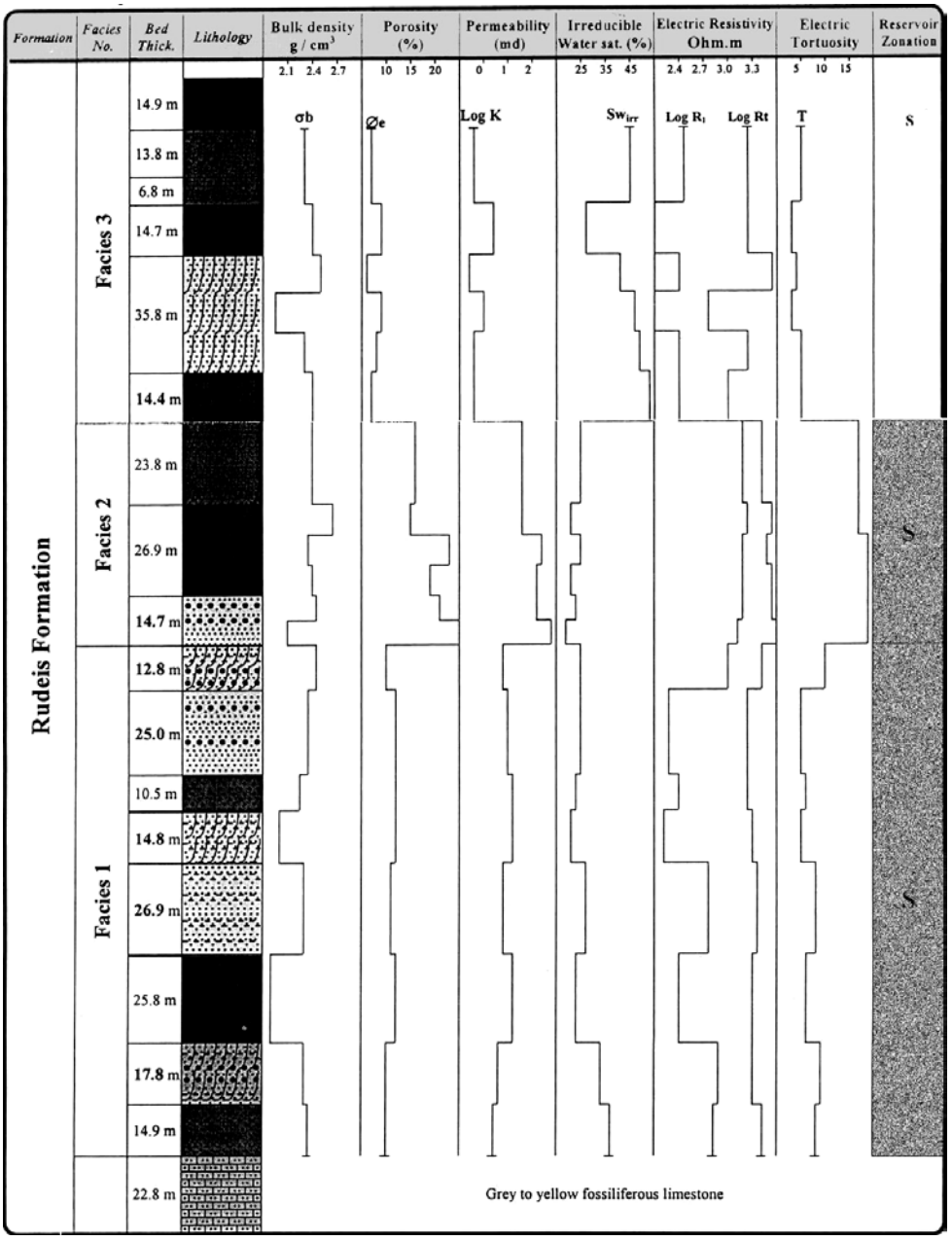

Fig. 9: Log chart showing the vertical variation of the different measured petrophysical parameters of the Lower Miocene Rudies Formation, Gebel Hadahid, Wadi Feiran, Sinai.

CONCLUSIONS

From the previous results and discussions, the following conclusions can be drawn:

1) Discriminating the studied rocks according to their measured petrophysical parameters leads to excellent correlation coefficients in the different x-y plots.

2) The calcareous sandstone rock samples of the Rudeis Formation in the studied section of Gebel Hadahid, Wadi Feiran, South West Sinai, could be differentiated into three petrophysical facies.

3) The lower and middle parts of Rudeis Formation (first and second facies of the studied section) have good storage capacity due to their high porosity and permeability, while the third facies has low storage capacity due to their poor porosity, low permeability values and due to the well and tight cementation.

4) Under the condition of similarity of the paleoenvironment of deposition and the diagenetic history, and taking into consideration the gradient of the geopressure, the lower and middle parts of Rudeis Formation in its subsurface extensions have good shows and reliability to contain economic

fluids in the presence of fluid supply and capturing conditions.

5) The multiplier (a) and the cementation exponent (m) of the different studied facies increase with increasing the solution salinity, and

6) The behaviour of the electric tortuosity factor of facies 2 with both the porosity and permeability is considered as a special case that could be attributed to increasing the values of pore channel diameter simultaneously with increasing values of the electric tortuosity factor of the studied rock samples.

REFERENCES

Abu El Enain, F.M. and Gharib, K.S. (1997): "Petrophysical facies analysis of the Miocene clastics exposed in Hadahid area, Sinai, Egypt", Egypt. J. Geol., vol. 1, no. 1, pp. 197-224.

Amyx, J.W., Bass, D.M. and Whiting, R.L. (1960): "Petroleum reservoir engineering", McGraw, Hill Book Co. Inc., New York, 610 p.

Arafa, A. (1992): "Nannoplanktons and planktonic foraminiferal zonation of the Lower Miocene sequence in Gebel Hadahid, South West Sinai, Egypt", Egypt. J. Geol., vol. 35 (1-2), pp. 275-284.

El Heiny, I. (1982): "Neogene stratigraphy of Egypt", Newesl. Straig., vol. 11, no. 2, pp. 41-54.

El Kerdany, M.T. (1976): "Note of the planktonic zonation of the Miocene in the Gulf of Suez region, U.A.R.", Com., Med.. Neog. Stratigraphy Proceeding, pp.157-166.

El Sayed, A.M.A. (1993): "Packing Index and saturation parameters for limestone", Ain Shams Science Bull., vol. 31, pp. 411-424.

El Sayed, A.M.A. and Zeidan, S. (1983): "Contribution to the formation resistivity factor-porosity relation", Proc. of 2nd Ann. Meeting of E.G.S., pp. 129-147.

El Sayed, A.M.A., El Batanony, M.H., Ali, Y.A. and El Naggar, O.M. (1999): "Effect of overburden pressure on cementation exponent; the Rudies Formation, Western Sinai, Egypt", Proc. of 17th Ann. Meeting of E.G.S., pp. 93-110.

Gür, A. M. (1976): "Petroleum engineering", Ferdinand Enke publishers, Stuttgart, 385 p.

Hamza, F. (1988): "Miocene litho- and biostratigraphy in west central Sinai, Egypt", M.E.R.C. Ain Shams Univ., Earth Sci. Ser., vol. 2, pp 91-103.

Heybroeak, F. (1965): "The Red sea Miocene evaporites basin, salt basins around Africa", Institute of Petroleum, London, Elsevier Publ. Co., Amsterdam, pp. 17-40.

Koithara, J., Hashmy, K. and Mehra, Y.M. (1968): "Report on the laboratory study of core samples from productive sandstones (Barails) in Rudrasafar field for establishing relationships between electrical and reservoir parameters", Unpublished report of the Institute of Petroleum Exploration, OWGC.

McQueen, H.S. (1931): "Insoluble residues as a guide in stratigraphic studies", Missouri. Geol. Surv., 56th Biemn Rept. State Geol., April, no. 1, pp. 103-131.

Parkhomenko, E.I. (1967): "Electric properties of rocks", Plenum Press, New York, 315 p.

Ragab, M.A., Khaled, Kh.A. and Nabawy, B.S. (1999): "Evaluation of surface Upper Eocene rocks as reservoir, Fayum, Egypt: sedimentary, petrophysical and magnetic study", J. Sed. Egypt, vol. 7, pp. 149-166.

Ragab, M.A., El Sayed, A.A. and Nabawy, B.S. (2000): "Physical parameters of Egyptian oil reservoir sedimentary rocks, A review: In Sedimentary Geology of Egypt, Applications and economics", S.M. Soliman (Ed.), part 1, pp. 129-150.

Rateb, R. (1988): "Miocene planktonic foraminiferal analysis and its stratigraphic application in the Gulf of Suez region", 9th EGPC Exploration and production Conference, Cairo, pp. 1-22.

Rzhevsky, Y. and Novik, G. (1971): "The physics of rocks", Translation and Edited by A. A. Beknazarov, Mir Publishers, Moscow, 320 p.

Sadek, A. (1968): "Contribution to the Miocene stratigraphy of Egypt by means of calcareous nannofossils", Rev. Espan. Micropaleontol., vol. 3, pp. 277-282.

Stainforth, R.M. (1949): "Foraminifera in the Upper Tertiary of Egypt", J. Paleo., vol. 23, pp. 385-392.